Earth, Moon, and Planets (2005) 97: 331–339
DOI 10.1007/s11038-006-9071-0

Pre-Impact Mid-IR and Optical Observations of Comet 9P/Tempel 1

H.-U. KAEUFL
European Southern Observatory, 85748, Garching bei Muenchen, Germany

T. BONEV
Institute of Astronomy Bulgarian Academy of Sciences, Tsarigradsko Chaussee 72, 1784, Sofia, Bulgaria
(E-mail: tbonev@astro.bas.bg)

H. BOEHNHARDT
Max Planck Institute for Solar System Research, 37191, Katlenburg-Lindau, Germany

Y. R. FERNANDEZ
Institute for Astronomy, University of Hawaii, Honolulu, USA

C. LISSE
University of Maryland, JHU-APL Baltimore, Baltimore, USA

(Received 20 November 2005; Accepted 17 March 2006)

Abstract. Comet 9P/Tempel 1, the target of the Deep Impact mission, has been intensively observed for a long time period before the encounter. Pre-impact ground based monitoring of the comet was an important prerequisite for the success of the first space experiment in which a comet is treated by an artificial impact. It provided the background data needed to disentangle the features caused by the impact from variations caused by the natural activity of the comet. In this paper we present results from the ESO-monitoring of the comet, conducted in the thermal infrared and optical spectral ranges during several months before the Deep Impact encounter with the comet.

Keywords: Comet 9P/Tempel 1, cometary dust, deep impact, optical imaging, thermal infrared

1. Introduction

We present observations of the dust coma of comet 9P/Tempel 1, the target of the Deep Impact mission. The observations were conducted between January and March 2005 at the La Silla site of ESO. Optical R-band images were obtained in January with SUSI2, and in February and March with EMMI at the NTT. Mid-infrared (MIR) images were acquired with TIMMI2 at the 3.6 m telescope simultaneously with the optical data in February and March. The MIR images were obtained at 7.9, 8.9, 9.8, 10.4, and

11.9 micron. The thermal infrared images are spatially resolved at sub-arcsec level. The optical images contain structures caused by dust emissions from discrete sources on the cometary nucleus. We first present the MIR images and analyse their morphology and fluxes. Then a description of the optical coma follows with discussion of the observed structures. At the end the MIR and optical data are combined to yield the albedo of the dust.

2. The Thermal Infrared Images

Comet 9P/Tempel 1, the target of the Deep Impact mission, was observed with the ESO TIMMI2 camera at the 3.6 m telescope of La Silla observatory on February 23 and March 25, 2005. Figure 1 shows the final calibrated images from March 25. A low-pass filter was applied to these images to reduce the background noise.

Basic data for the mid-IR images are summarized in Table I. The geometrical conditions during the time of observations can be found in Table II which contains the description of the simultaneously obtained optical images. The angular size of the TIMMI2 pixel is 0.2″/px,[1] which yields a projected spatial scale at the comet of 165 and 122 km/px for the observations on Feb 23 and March 25, respectively. The images were calibrated to W m^{-2} μm per pixel by using measurements of the standard star HD 123139 obtained at similar airmass immediately after the observations of the comet. The weather conditions were stable, with a PSF FWHM = 0.75″ for all wavelengths, measured in the standard star's images. The dust coma in the presented thermal IR images is resolved at subarcsecond level. This is illustrated with the growth curves shown in Figure 2. For the data obtained on Feb 23 (left panel) the spatial resolution is reliable only in the inner 1 arcsec (≤1000 km). On March 25 (right panel) the dust coma is extending to distances greater than 4 arcsec (≥2000 km) from the central condensation. In February the comet differs from a point source, but the S/N is much lower as compared to March. The comet was too faint in February. In the best cases (10.4 and 11.9 μm) the signal at the nucleus is about 3-σ above the background noise and reaches the background level at a distance of about 5 px (= 830 km). The shallower profile in February is real in the confidence limits given by the error bars in the left panel of Figure 2.

The left panel in Figure 3 shows the spectral energy distribution (SED) in the mid-infrared range. It was derived from the images obtained on March 25 by integrating the surface brightness in a circular aperture of radius 1″, centred at the position of the brightest point in the inner dust coma. The error bars show the 3σ confidence level of the measured data. The tail of the

[1] Data concerning the instrumentation can be found in http://www.ls.eso.org/lasilla/sciops/3p6/timmi/

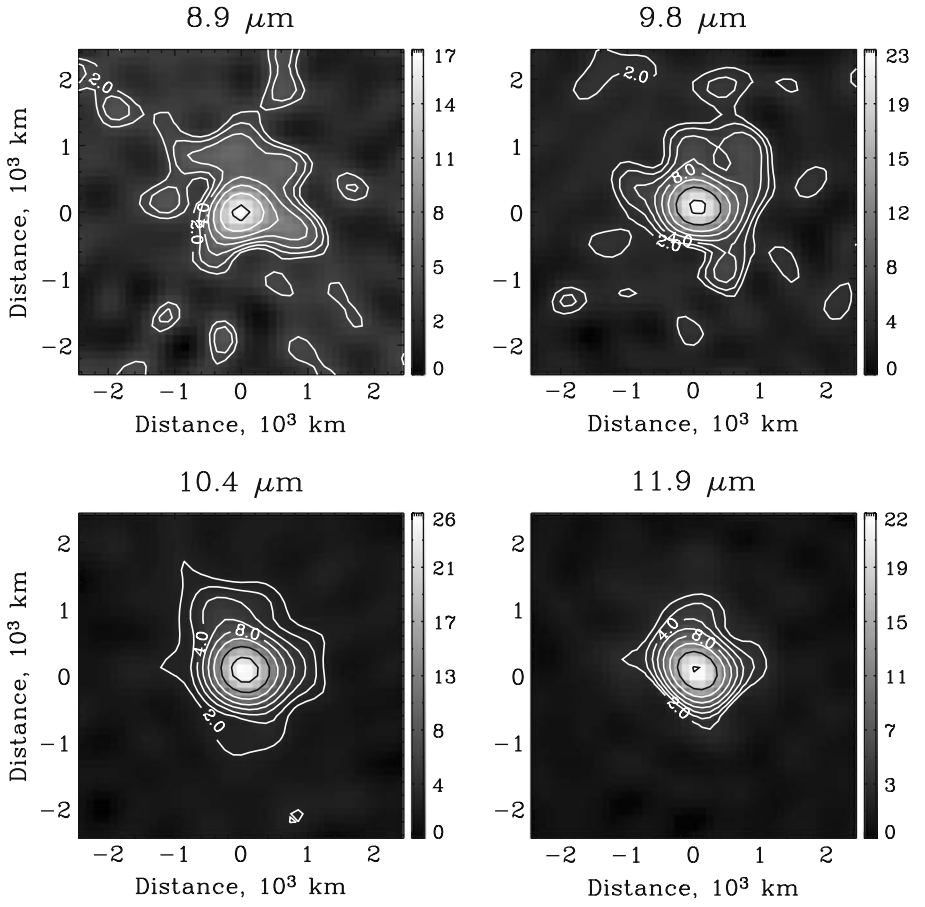

Figure 1. Thermal infrared images of comet 9P/Tempel 1 obtained with TIMMI2 at 4 wavelengths in the N-band on March 25, 2005. North is down and East to the right. The direction to the Sun is projected in the lower right part of the images, at 52° from North to East. The thermal surface brightness of the images is coded in grey levels as shown in the scale bar to the right of the images. The units are 10^{-17} W m^{-2} μm per pixel.

TABLE I
Data for the MIR observations of comet 9P/Tempel 1

Date	From UT to UT	Filters at λ, μm	Airmass range
2005/02/23	6:33–8:23	11.9, 10.4, 9.8, 8.9, 7.9	1.4–1.3
2005/03/25	7:32–9:24	11.9, 10.4, 9.8, 8.9, 7.9	1.5–2.4

arrow is placed at 1-σ of the background noise measured in the image taken at 7.9 μm. No signature of the comet could be detected at this wavelength. The purpose of the arrow is to indicate a possible upper limit for the flux of the comet at 7.9 μm. A fit to the data with blackbody radiation yields a

TABLE II
Conditions and parameters of the optical observations

Date[a] Date, from UT to UT	r[b] AU	Δ[c] AU	Instrument	Scale ″/px, km/px	ϕ[d] degree	α[e] degree
2005 Jan 23, 6:47–7:49	2.14	1.57	SUSI2@NTT	0.0805, 92	25.3	287.5
2005 Feb 23, 7:59–9:23	1.97	1.14	EMMI@NTT	0.1665, 138	20.7	274.1
2005 Mar 25, 7:52–9:24	1.81	0.84	EMMI@NTT	0.1665, 101	12.1	231.8

[a]The times give the start and end of a series of images obtained in the corresponding night.
[b]Heliocentric distance.
[c]Geocentric distance.
[d]Phase angle.
[e]Position angle of the extended Sun–Comet radius vector.

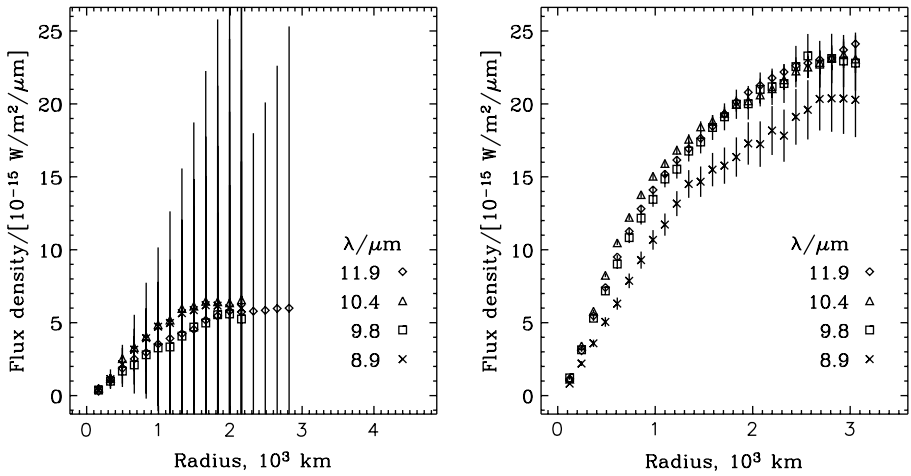

Figure 2. Curves of growth derived from the calibrated thermal infrared images. Left: Feb 23, 2005. Right: Mar 25, 2005.

temperature of 230 ± 15 K, which is about 10% greater than the equilibrium temperature of a black or grey body at the heliocentric distance of the comet. We adopted the fitted blackbody spectral distribution as a continuum which was used to produce the relative fluxes presented in the right panel of Figure 3.

3. The Optical Images

Optical observations were performed in 3 epochs, separated by roughly 1 month. Detailed information on the observational circumstances is given in

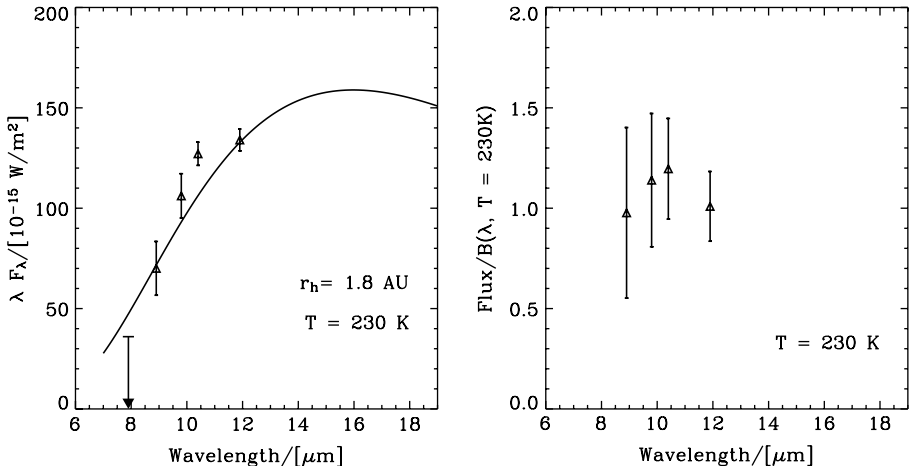

Figure 3. Left: The spectral energy distribution as derived from the observations on March 25. The data points are fluxes integrated in aperture of radius 1″ in the images taken at different wavelength. The full line is a fit to the data with a 230 K black body radiation. Right: The spectral energy distribution divided by the "continuum." The blackbody radiation with temperature 230 K, fitted to the data in the left panel, served as a "continuum" for this normalization.

Table II. The February and March images were calibrated to W m^{-2} μm by using measurements of several standard stars in 2 fields (Landolt, 1992) obtained at different airmasses. Because of the non-photometric conditions during the observations in January we are using these images only for morphological analysis.

Figures 4, 5, and 6 show contour plots of the surface brightness distributions as derived from the observations obtained on Jan 23, Feb 23, and Mar 25, respectively. The right panels in these figures contain the original images multiplied with the distance to the photocentre, ρ. This technique removes the mean ρ^{-1} brightness decrease which is expected close to the nucleus in the case of stationary isotropic dust outflow. Thus, structures which are deviating from the expected mean brightness distribution are enhanced. A well expressed straight jet is seen in the February and March images, at position angles $220° \pm 5°$, and $215° \pm 5°$, respectively (Kaeufl et al., 2005). The structure observed in March is close to the antisolar direction, and the question arises if it not merely represents the main stream of the dust tail. There are several arguments against this suspicion. The dust tail should extend between the antisolar direction and the negative velocity vector. The observed structure extends at more than 15° apart from the antisolar direction, but its dislocation is in the "wrong" direction. Furthermore, the structure-to-total brightness ratio, calculated in the inner coma (aperture radius 5000 km), is about 0.1% and does not change from February to

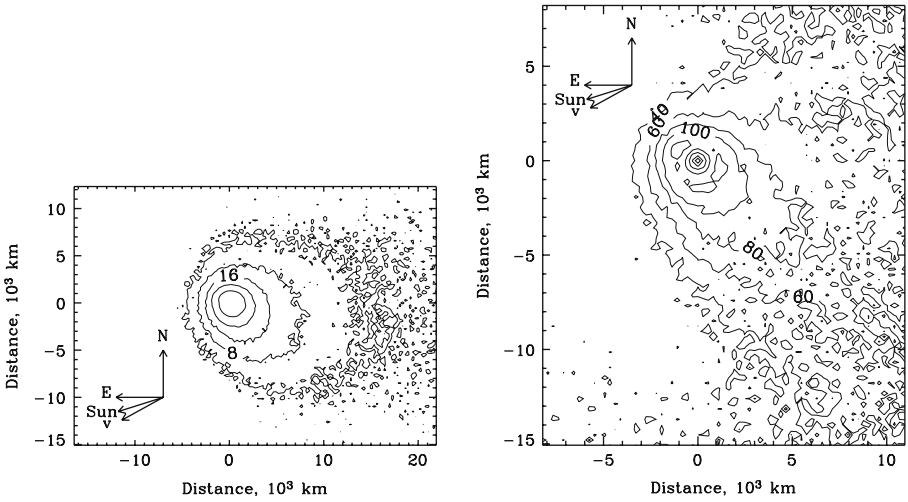

Figure 4. Left: Surface brightness of comet 9P/Tempel 1 in the R-band as observed with SUSI2 on January 23, 2005. The image is a composite of 24 frames with a total exposure of 12 min (24 frames × 30 s). Right: The image in the left panel was multiplied by ρ, the distance between the photocentre and any particular pixel. This normalization removes the mean $1/\rho$ brightness decrease and thus reveals faint structures in the inner bright dust coma. The arrows v and Sun show the projection of the heliocentric velocity vector and the projected direction to the Sun, respectively.

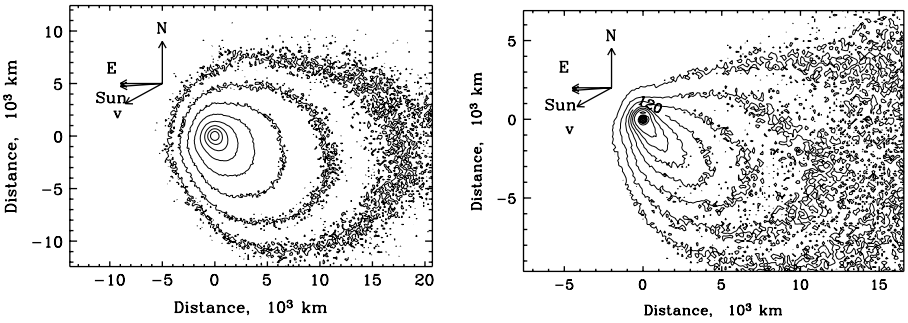

Figure 5. Left: Surface brightness of comet 9P/Tempel 1 in the R-band as observed with EMMI on February 23, 2005. The image is a composite of 61 frames with a total exposure of 2440 s (61 frames × 40 s). The contours are spaced by a factor of 2, starting outward at a level of 0.5×10^{-18} W m^{-2} μm which is equal to 5σ of the background noise. Right: Same as in Figure 4.

March. In January there is no well expressed structure, but the inner dust distribution is extended at 228° ± 5°, far from the almost 290° position angle of the antisolar direction (q.v. Table II). In the three cases the projected orientation of the structure is approximately perpendicular to the projected orbital motion of the comet. This suggests that the jet lies in a plane which is close to perpendicular to the orbital plane of the comet. Sekanina (1987)

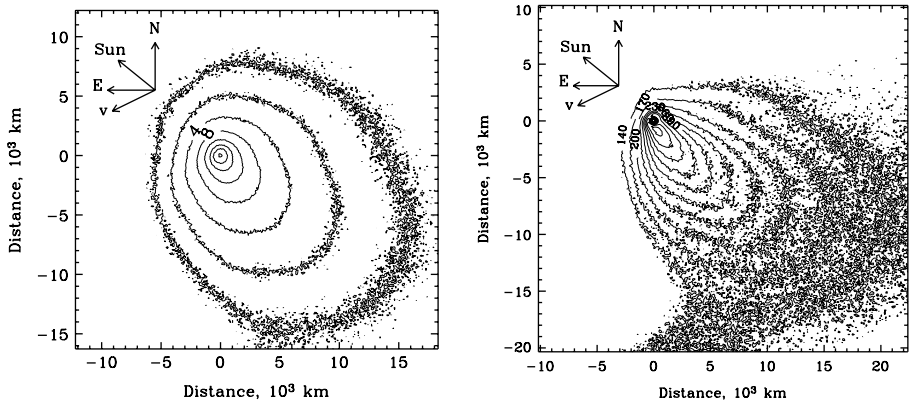

Figure 6. Left: Same as Figure 5 but for the observations on March 25, 2005. The image is a composite of 71 frames with a total exposure of 2820 s (2 frames × 30 s + 69 × 40 s). The contours are spaced by a factor of 2, starting outward at a level of 1.0×10^{-18} W m^{-2} μm which is equal to 5σ of the background noise. Right: Same as Figure 4.

shows that source regions located near the equatorial plane of a comet produce spiral jets, and that such jets vary dramatically from day to day. In our case the structure does not show any curvature up to projected distances of about 10^4 km. This is an indications that the source of the observed structure should be located at large cometographic latitudes. In such a case the direction of the jet approximates the projected position of the rotational axis. We can conclude that the spin vector of the nucleus should lie in a plane close to perpendicular to the orbital plane of the comet. Figure 7 shows the mean brightness decrease as derived by averaging the surface brightness in azimuthal direction. A power law was fitted to the particular mean profiles. The comparison between the three epochs shows a systematic increase of the power index from −1.8, through −1.7, to −1.4. On April 14, 2005 Lara et al. (2005) observed comet Tempel 1 and measured radial-brightness profiles following a power law with indices between −1.30 and −1.47 in the north-south direction.

We derived values of Afρ (A'Hearn et al., 1984) of 124 ± 30 cm and 176 ± 10 cm on Feb 23 and Mar 25, respectively. These values fit well to the pre-perihelion raising wing of Afρ-values, found by other observers during several previous perihelion passages of the comet and summarized in Lisse et al. (2005). The values of Afρ should be independent on the aperture size in the case of a stationary radial outflow. Under these idealized conditions the brightness profile should follow a power law with slope = −1.0, given on Figure 7 with the dotted lines. The same figure shows that the observed brightness decrease deviates strongly from the expected under stationary conditions. Therefore the calculated Afρ-values will be dependent on the size of the aperture used. The above given values refer to flux measurements in a

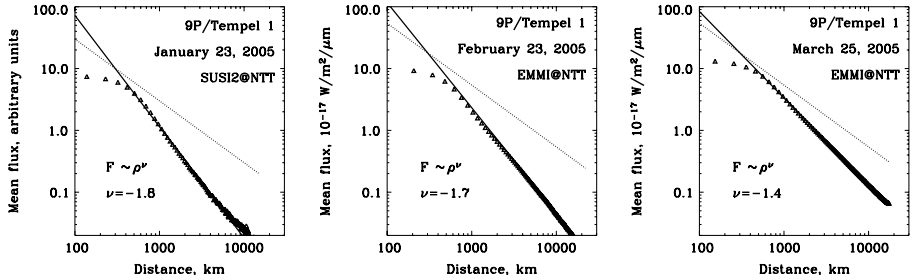

Figure 7. Azimuthally averaged mean profiles for the 3 epochs of observations in the R-band. The full line is the best fit to the data with a power law. The slope of the power law is indicated in the panels. The dotted line shows a power law with slope = −1.0.

synthetic aperture of radius 5″. Arpigny has found an empirical correlation between values of Afρ and the production of dust (A'Hearn et al., 1995). Following his empirical rule we derive a rough estimation of 200 kg s^{-1} for the dust production of comet Tempel 1 on Mar 25, 2005.

4. Combined Analysis of the IR and Optical Data

Simultaneous thermal IR and optical measurements allow to derive the grain albedo, A (O'Dell, 1971). The total energy scattered and the total energy absorbed (and radiated) are related to the albedo, by following equation (Ney, 1982):

$$\frac{(\lambda F_\lambda)_{\mathrm{maxVIS}}}{(\lambda F_\lambda)_{\mathrm{maxIR}}} = \frac{A}{1-A}. \tag{1}$$

The successful application of this relation depends on how well the data can be fitted by a blackbody radiation. Using our SED from March 25 and the range of temperatures found for the IR radiation (see Figure 3) we derive values for the albedo in the range 0.07–0.11. Lisse et al. (2005) have used IRAS measurements in the range 8–100 μm in combination with contemporaneously obtained narrow-band continuum data at 5240 Å and derived an albedo of 8 ± 2%. The measurements used by Lisse et al. (2005) were obtained in July–August 1983. The albedo of the dust grains in comet 9P/Tempel seems to be unchanged over the last 22 years.

5. Conclusions

We have presented thermal infrared and optical observations of comet 9P/Tempel 1 obtained during the ESO pre-Deep Impact monitoring program of

this comet. We found that the comet closely resembles the characteristics derived from several previous apparitions during the last 22 years. The albedo of its dust grains is between 7% and 11%. Three months before perihelion its dust production was about 200 kg s^{-1}. The morphology of the dust coma is characterized by the existence of at least one strong jet. The shape and the orientation of this jet suggest that its source is located at high cometographic latitudes.

Acknowledgements

T.B. gratefully acknowledges a fellowship from the Scientific Visitor Programme of the European Southern Observatory. This research was partially supported by contract Φ-1009 with the Ministry of Education and Science, Bulgaria. Critical remarks by two reviewers helped to improve the quality of this paper.

References

A'Hearn, M. F., Millis, R. L., Schleicher, D. G., Osip, D. J., and Birch, P. V.: 1995, *Icarus* **118**, 223–270.

A'Hearn, M. F., Schleicher, D. G., Millis, R. L., Feldman, P. D., and Thompson, D. T.: 1984, *AJ* **89**, 579–591.

Kaeufl, H. U., Bonev, T., Boenhardt, H., Fernandez, Y. R., and Lisse, C.: 2005, *IAU Circ.* **8539**, 1.

Landolt, A. U.: 1992, *AJ* **104**, 340–371.

Lara, L. -M., Boehnhardt, H., Gredel, R., Gutierrez, P. J., Ortiz, J. -L., Rodrigo, R., and Jesus Vidal-Nunez, M.: 2005, *IAU Circ.* **8532**, 2.

Lisse, C. M., A'Hearn, M. F., Farnham, T. L., Groussin, O., Meech, K. J., Fink, U., and Schleicher, D. G.: 2005, *Space Sci. Rev.* **117**, 161–192.

Ney, E. P.: 1982, in L. L. Wilkening (ed.), *Comets. University of Arizona press*, Tucson, AZ, pp. 323–340.

O'Dell, C. R.: 1971, *ApJ* **166**, 675.

Sekanina, Z.: 1987, in E. J. Rolfe and B. Battrick (eds.), *Proceedings of International Symposium on Diversity and Similarity of Comets*, ESASP-278, pp. 315–322.